Toca-1 Mediates Cdc42-Dependent Actin Nucleation by Activating the N-WASP-WIP Complex

Hsin-Yi Henry Ho,[1,3] Rajat Rohatgi,[1,3,4]
Andres M. Lebensohn,[1] Le Ma,[1,5] Jiaxu Li,[2]
Steven P. Gygi,[2] and Marc W. Kirschner[1,*]
[1]Department of Systems Biology
[2]Department of Cell Biology
Harvard Medical School
Boston, Massachusetts 02115

Summary

An important signaling pathway to the actin cytoskeleton links the Rho family GTPase Cdc42 to the actin-nucleating Arp2/3 complex through N-WASP. Nevertheless, these previously identified components are not sufficient to mediate Cdc42-induced actin polymerization in a physiological context. In this paper, we describe the biochemical purification of Toca-1 (*trans-ducer of C*dc42-dependent *a*ctin assembly) as an essential component of the Cdc42 pathway. Toca-1 binds both N-WASP and Cdc42 and is a member of the evolutionarily conserved PCH protein family. Toca-1 promotes actin nucleation by activating the N-WASP-WIP/CR16 complex, the predominant form of N-WASP in cells. Thus, the cooperative actions of two distinct Cdc42 effectors, the N-WASP-WIP complex and Toca-1, are required for Cdc42-induced actin assembly. These findings represent a significantly revised view of Cdc42-signaling and shed light on the pathogenesis of Wiskott-Aldrich syndrome.

Introduction

The actin cytoskeleton drives dynamic cellular processes such as cell motility, cytokinesis, and vesicular movement. The proper execution of these complex processes requires that cells integrate intra- and extracellular signals to control actin assembly (and disassembly) with a high degree of temporal and spatial specificity. Phosphoinositides and members of the Rho family of small GTP binding proteins, whose founding members include Rac, Rho, and Cdc42, have been implicated as important signaling intermediates that link cell surface signals to the actin cytoskeleton (Etienne-Manneville and Hall, 2002; Yin and Janmey, 2003). Over the past decade, a great deal of effort has focused on identifying the pathways that link Rho family GTPases and phosphoinositides to the control of actin polymerization.

We have successfully used cytoplasmic extracts made from *Xenopus* eggs to investigate how the Rho family protein Cdc42 regulates actin nucleation (Ma et al., 1998a). These extracts faithfully recapitulate the cel-lular cytoplasmic milieu. Actin polymerization is globally inhibited but can be locally activated by signals such as activated Cdc42 or phosphatidylinositol 4,5-bisphosphate (PIP_2) (Ma et al., 1998a). Our prior work in high-speed supernatant fractions of *Xenopus* egg extracts (called "*Xenopus* HSS" throughout the text) has delineated an actin nucleation pathway composed of PIP_2, Cdc42, N-WASP, and the Arp2/3 complex (Ma et al., 1998b; Rohatgi et al., 1999). Using purified components, we showed that Cdc42 and PIP_2 can synergistically activate N-WASP, which in turn stimulates the actin-nucleating activity of the Arp2/3 complex (Rohatgi et al., 1999). (This system will be referred to as the "purified system" throughout the text.) This work, along with work in several other systems, converged to demonstrate that the WASP family of proteins relays signals from Rho family GTPases to actin nucleation through the Arp2/3 complex (Machesky et al., 1999; Rohatgi et al., 1999). In addition to the ubiquitously expressed N-WASP, the WASP family includes the founding member Wiskott-Aldrich syndrome protein (WASP), mutated in the eponymous pediatric disease, and the Scar/WAVE proteins, implicated in linking the Rac pathway to the Arp2/3 complex (Derry et al., 1994; Miki et al., 1998).

Given that WASP family proteins function as integration nodes for signals to the Arp2/3 complex, it is important to understand how these proteins are themselves regulated. Biochemical and structural studies of WASP/N-WASP have shown that these molecules exist in an autoinhibited conformation, in which the N-terminal regulatory domain blocks the activity of the C-terminal Arp2/3 activating domain (Kim et al., 2000; Rohatgi et al., 2000). Under purified conditions in vitro, this autoinhibitory interaction can be relieved by a myriad of potential upstream activators, including Cdc42, PIP_2, Src-homology 3 (SH3) domain containing proteins such as Nck and Grb2, and tyrosine kinases (Carlier et al., 2000; Cory et al., 2003; Rohatgi et al., 1999, 2001; Suetsugu et al., 2002; Torres and Rosen, 2003). Nevertheless, it is not clear which activators are physiologically important.

Despite the insights gained by studying N-WASP under purified conditions, there are important differences between the previously described purified system and the more physiological *Xenopus* extract system. First, while activated Cdc42 alone is sufficient to induce robust actin polymerization in the putatively lipid-free *Xenopus* HSS (which is a 100,000 × g supernatant), both Cdc42 and PIP_2 are required for the full activation of N-WASP in the purified system (Rohatgi et al., 1999). This suggests that additional factor(s) control N-WASP activation in extracts. Second, most of the N-WASP in extracts is in a complex with WIP (WASP interacting protein) or a related protein, CR16, rather than as free N-WASP (Ho et al., 2001). We suspected that the N-WASP-WIP/CR16 complex might have a different mode of regulation from that of free N-WASP, as observed in the purified system. Finally, a PIP_2 binding mutant of N-WASP that cannot respond to PIP_2 in the purified system is capable of partially rescuing PIP_2-induced actin polymerization in N-WASP-depleted ex-

*Correspondence: marc@hms.harvard.edu
[3]These authors contributed equally to this work.
[4]Present address: Department of Oncology, Stanford University Medical Center, Stanford University, Stanford, California 94305.
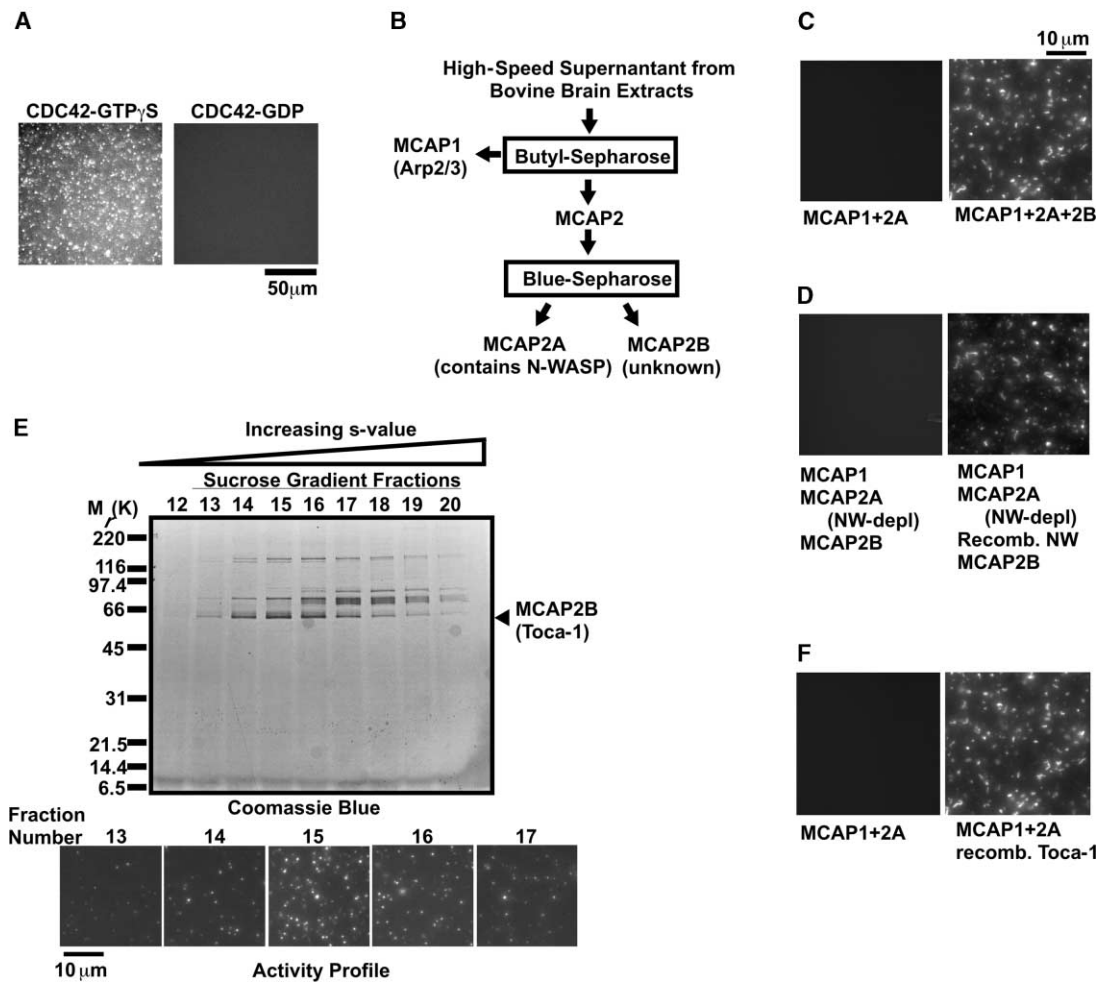[5]Department of Biological Sciences, Stanford University, Stanford, California 94305.

Figure 1. Biochemical Purification of Toca-1

(A) Cdc42-induced F-actin foci formation. High-speed supernatants (HSS) made from brain extracts were supplemented with rhodamine-actin (3 μM) and either activated (GTPγS loaded) or inactive (GDP loaded) Cdc42. The formation of F-actin foci was assayed by fluorescence microscopy.

(B) Fractionation scheme used for the separation of three MCAP (*mediators of Cdc42-dependent actin polymerization*) activities from bovine brain HSS.

(C) All three MCAPs are required to reconstitute Cdc42-induced actin polymerization. MCAP1 (in the form of purified Arp2/3 complex) and MCAP2A (a crude fraction containing N-WASP) are not sufficient.

(D) N-WASP is an essential component of MCAP2A. Cdc42-induced actin assembly is abolished by immunodepletion of N-WASP from MCAP2A (left panel) but can be rescued by purified N-WASP (50 nM N-WASP, right panel).

(E) Active fractions from the final sucrose gradient step of MCAP2B purification were analyzed by SDS-PAGE. The activity profile across the sucrose gradient is shown below the gel. MCAP2B activity perfectly cofractionated with an ~60 kDa protein band (indicated by an arrowhead) in the gel.

(F) Purified recombinant human Toca-1 fully complements the activity of MCAP2B in the Cdc42-induced F-actin foci formation assay.

tracts, suggesting that the major function of PIP_2 in extracts is not at the level of N-WASP activation, as suggested by the purified system (Rohatgi et al., 2000). These observations indicate that the previously described purified system (consisting of Cdc42, PIP_2, free N-WASP, and the Arp2/3 complex) is incomplete.

In order to better understand the Cdc42 pathway, we fractionated *Xenopus* HSS with the goal of identifying all of the required components. In this paper, we report the purification of an essential component called Toca-1 (*transducer of Cdc42-dependent actin* assembly) to ho-

mogeneity. The importance of Toca-1 is underscored by the finding that it is also required both for PIP_2-induced actin polymerization and for the actin-driven motility of endomembrane vesicles. Toca-1 is a Cdc42 binding protein and is a member of the PCH (*pombe Cdc15 homology*) protein family highly conserved across eukaryotes (Lippincott and Li, 2000). Based on analysis of interactions between Toca-1 and the previously described components, we construct a revised model of this important pathway. This model substantially clarifies the molecular logic of Cdc42-actin signaling, suggests a

Table 1. Purification Table for MCAP2B

Fraction	Activity (unit)	Protein (mg)	Specific Activity (unit/mg)	Fold Purification	Yield (%)
High-speed supernatant	—	30,000	—	—	—
Butyl eluate	200,000	3600	56	1	100
Resource S	100,000	200	500	9	50
Cibacron blue	80,000	70	1140	20	40
Superose 6	40,000	21	1900	35	20
Mono Q	30,000	4	7500	135	15
Mono S	12,000	0.3	40,000	720	6
Mini S	6000	0.15	40,000	720	3
Sucrose gradient	4000	0.015	270,000	4800	2

Starting material, 25 bovine calf brains. Activity unit is defined by the amount (volume) of MCAP2B-containing fraction required to support Cdc42-induced actin foci formation in a $7\mu L$ reaction volume. Given that the microscopic assay described in Figure 1 is inherently qualitative, the activity levels are estimated based on end-point dilution and a four-point visual scoring system. Activity in the high-speed supernatant was too low to be assayed quantitatively and thus was not included in the computation of final fold purification. If this step is included, we estimate the net purification to be at least 25,000-fold.

biochemical function for the emerging PCH family of proteins, and provides insights into the molecular pathogenesis of Wiskott-Aldrich syndrome.

Results

A Previously Unidentified Activity Is Required for Cdc42-Dependent Actin Assembly in Cell Extracts

We previously reported the reconstitution of Cdc42-induced actin assembly in high-speed supernatants made from *Xenopus* egg extracts ("*Xenopus* HSS") (Ma et al., 1998a). The Arp2/3 complex and N-WASP are two components essential for this activity; however, one additional chromatographically distinct activity is also required. In developing a purification strategy, we discovered that this activity could be more easily isolated from bovine brain extracts. As the *Xenopus* HSS is much more amenable to quantitative monitoring of actin assembly, we return to it after the purification for biochemical analysis of the pathway.

High-speed supernatants made from bovine brain extracts (brain HSS) behave much like *Xenopus* HSS with respect to actin assembly. Actin polymerization is initiated by the addition of recombinant Cdc42-GTPγS to brain HSS supplemented with rhodamine-labeled actin, resulting in the rapid formation of F-actin (cytochalasin B-sensitive) foci (Figure 1A). As expected, the activity depends on the GTP bound state of Cdc42. This pathway is also specific to Cdc42. Other small G proteins such as Rac and Rho cannot induce F-actin foci (data not shown). This rhodamine-actin based microscopic assay is quick and consumes only a small amount of material, making it an ideal assay for following the activity of this pathway during protein purification.

As in the *Xenopus* system, fractionation of bovine brain HSS revealed that Cdc42-induced actin polymerization requires at least three chromatographically distinct activities, or MCAPs (*m*ediators of *C*dc42-induced actin *p*olymerization) (Figures 1B and 1C) (Ma et al., 1998b). We have previously described the purification of MCAP1 as the Arp2/3 complex (Ma et al., 1998b; Rohatgi et al., 1999). α-N-WASP immunoblotting revealed that the majority of N-WASP cofractionated with

MCAP2A (data not shown). Immunodepletion of N-WASP from MCAP2A eliminated the ability of MCAP2A to support Cdc42-induced actin assembly when combined with the Arp2/3 complex and MCAP2B (Figure 1D). The activity could be restored by adding recombinant N-WASP to the depleted fraction (Figure 1D). Thus, in agreement with our prior results in the *Xenopus* system (Rohatgi et al., 1999), N-WASP is an essential component of MCAP2A.

We next focused on the identification of MCAP2B, an activity that likely represented a previously unknown component of the Cdc42 pathway, as it did not cofractionate with either the Arp2/3 complex or N-WASP (Figure 1C). Early on in the purification, we noticed that the activity in MCAP2B had affinity for Cdc42. The activity can be depleted from MCAP2B fractions by Cdc42-GTPγS beads but not Cdc42-GDP beads (data not shown). Yet, attempts to identify MCAP2B by screening for known Cdc42 binding proteins or by affinity purification using immobilized Cdc42 were not successful. Therefore, we attempted to purify MCAP2B to homogeneity by conventional fractionation techniques.

Purification of MCAP2B from Bovine Brain Extracts

To purify MCAP2B, soluble proteins derived from 25 bovine calf brains were sequentially fractionated over eight steps shown in Table 1. At each step, column fractions were tested for their ability to support the formation of Cdc42-induced F-actin foci by combining them with purified Arp2/3 complex (MCAP1) and partially purified MCAP2A (as shown in Figure 1C). Throughout the entire purification, α-Arp3 and α-N-WASP immunoblotting was performed to confirm that MCAP2B was distinct from these previously identified components (data not shown).

After an estimated 25,000-fold purification, summarized in Table 1, the MCAP2B activity perfectly cofractionated with an ∼60 kDa protein (Figure 1E), which was unambiguously identified by liquid chromatography-coupled tandem mass spectrometry (LC/MS/MS). Twenty-three tryptic peptides matched an unnamed putative human protein product encoded by Sequence 3 from Patent WO0075321 (GenBank accession number AX058596_1) with a predicted molecular weight of 63
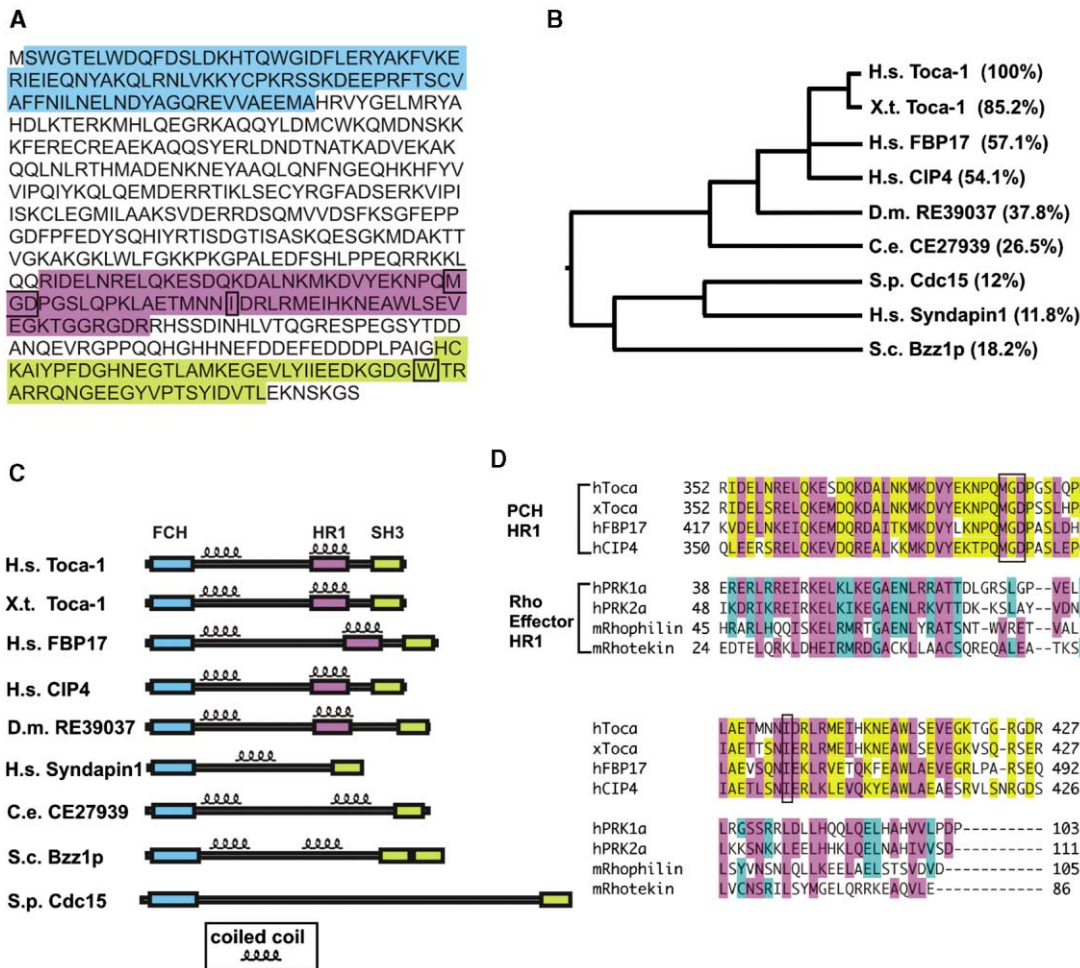
A

MSWGTELWDQFDSLDKHTQWGIDFLERYAKFVKE
RIEIEQNYAKQLRNLVKKYCPKRSSKDEEPRFTSCV
AFFNILNELNDYAGQREVVAEEMAHRVYGELMRYA
HDLKTERKMHLQEGRKAQQYLDMCWKQMDNSKK
KFERECREAEKAQQSYERLDNDTNATKADVEKAK
QQLNLRTHMADENKNEYAAQLQNFNGEQHKHFYV
VIPQIYKQLQEMDERRTIKLSECYRGFADSERKVIPI
ISKCLEGMILAAKSVDERRDSQMVVDSFKSGFEPP
GDFPFEDYSQHIYRTISDGTISASKQESGKMDAKTT
VGKAKGKLWLFGKKPKGPALEDFSHLPPEQRRKKL
QQRIDELNRELQKESDQKDALNKMKDVYEKNPQM
GDPGSLQPKLAETMNNIDRLRMEIHKNEAWLSEV
EGKTGGRGDRRHSSDINHLVTQGRESPEGSYTDD
ANQEVRGPPQQHGHHNEFDDEFEDDDPLPAIGHC
KAIYPFDGHNEGTLAMKEGEVLYIIEEDKGDGWTR
ARRQNGEEGYVPTSYIDVTLEKNSKGS

B

C

D

Figure 2. Toca-1 Belongs to the PCH Protein Family and Is Highly Conserved Across Eukaryotes

(A) The amino acid sequence and domain structure of human Toca-1. The FCH domain is highlighted blue, the HR1 domain purple, and the SH3 domain yellow.

(B) Phylogenetic analysis of Toca-1 and other PCH family proteins. H.s., *Homo sapiens*; X.t., *Xenopus tropicalis*; D.m., *Drosophila melanogaster*; C.e., *Caenorhabditis elegans*; S.c., *Saccharomyces cerevisiae*; S.p., *Schizosaccharomyces pombe*. Percent sequence identity to human Toca-1 for each protein is shown in parentheses.

(C) Schematic representation of Toca-1 and other PCH proteins showing their domain organization.

(D) Comparison of HR1 domains from PCH family proteins and from selected RhoA binding proteins. Residues similar among all HR1 domains are highlighted purple, residues similar among PCH proteins are highlighted yellow, and residues similar among RhoA binding proteins are highlighted blue. The MGD, I, and W residues mutated in the Cdc42- and N-WASP binding mutants of Toca-1 are boxed in (A) and (D).

kDa. We named this protein Toca-1 for *transducer of Cdc42-dependent actin assembly-1* (Figure 2A).

To confirm the nucleotide sequence encoding human Toca-1, we sequenced four independent PCR products derived from human fetal brain cDNA pools. All four sequencing reactions yielded identical sequences, which differed from that of Patent WO0075321 at ten different nucleotide positions. Our nucleotide sequence (deposited in GenBank as accession number AY514449) is more likely the accurate one, because it was derived from four independent cDNA amplification and sequencing reactions. Molecular cloning of Toca-1 was quite difficult because the cDNA encoding human Toca-1 is lethal to *E. coli*, and initially we were unable to express the protein. We overcame this difficulty by introducing silent mutations into the Toca-1 cDNA (described in Supplemental Data at http://www.cell.com/cgi/content/full/118/2/203/DC1).

After cloning Toca-1, we produced recombinant human Toca-1 in insect (SF9) cells (Figure 3B) and found that this protein could fully complement the bovine MCAP2B activity (Figure 1F). Thus, Toca-1 is responsible for the activity of MCAP2B.

Toca-1 Belongs to the PCH Protein Family and Is Conserved Across Eukaryotes

Sequence analysis revealed that Toca-1 is structurally related to proteins of the PCH (*pombe* Cdc15 *homology*) family, which have been implicated recently in a wide variety of actin-dependent processes, including cytoki-
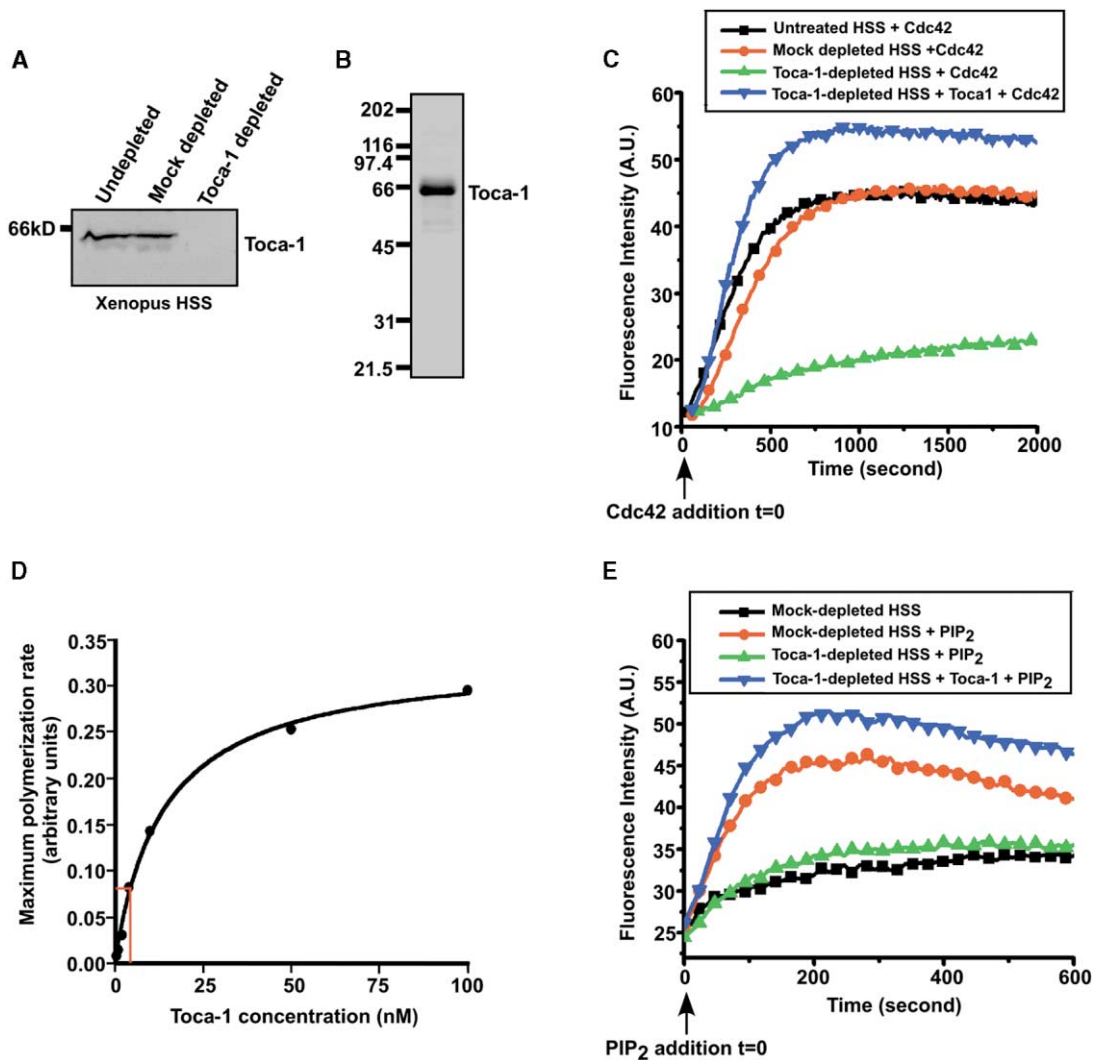
Figure 3. Toca-1 Is Required for Cdc42- and PIP₂-Induced Actin Assembly in *Xenopus* Egg Extracts

(A) Immunodepletion of Toca-1 from *Xenopus* HSS. Extracts were immunodepleted with α-Toca-1 or nonspecific (mock) antibodies and analyzed by α-Toca-1 immunoblotting.

(B) A purified preparation of recombinant human Toca-1 analyzed by SDS-PAGE and Coomassie blue staining.

(C) Comparison of actin assembly stimulated by Cdc42-GTPγS (250 nM) in untreated HSS, mock-depleted HSS, Toca-1-depleted HSS, and Toca-1-depleted HSS reconstituted with 5 nM recombinant Toca-1. Polymerization kinetics were monitored in the HSS using the pyrene-actin assay.

(D) Dose-response curve showing the variation in the maximum actin polymerization rate as a function of increasing concentrations of Toca-1 added back to Toca-1-depleted HSS. The maximum polymerization rate was calculated from the linear phase of polymerization curves of the type shown in (C). The curve is a nonlinear least squares fit of a single-site binding isotherm to the data points. The red lines denote the rate of filament elongation in untreated HSS stimulated with the same concentration of Cdc42.

(E) Comparison of actin assembly stimulated by PIP₂-containing vesicles (10 μM) in mock-depleted HSS, Toca-1-depleted HSS, and Toca-1-depleted HSS rescued with 10 nM recombinant Toca-1.

nesis, membrane trafficking, and cellular morphogenesis (Lippincott and Li, 2000). This protein family is conserved throughout eukaryotic evolution and includes human formin binding protein 17 (FBP17), human Cdc42-interacting protein 4 (CIP4), human syndapins, *D. melanogaster* RE39037, *C. elegans* CE27939, *S. cerevisiae* Bzz1p, and *S. pombe* Cdc15 (Figure 2B). Members of this protein family are defined by a common domain structure that includes a FER/CIP4 homology (FCH) domain at the N terminus and one or two Src homology 3

(SH3) domains at the C terminus (Figure 2C) (Lippincott and Li, 2000). The FCH domain is found in a large number of proteins involved in signal transduction, but its function is largely unknown. In addition, many PCH proteins are also predicted to contain coiled-coil domains. In the case of Toca-1, FBP17, CIP4, and *D. melanogaster* RE39037, one of these coiled-coil regions has homology to a domain called HR1 (protein kinase C-related kinase *h*omology *r*egion 1), which was originally identified as a Rho-interactive module in several RhoA binding proteins
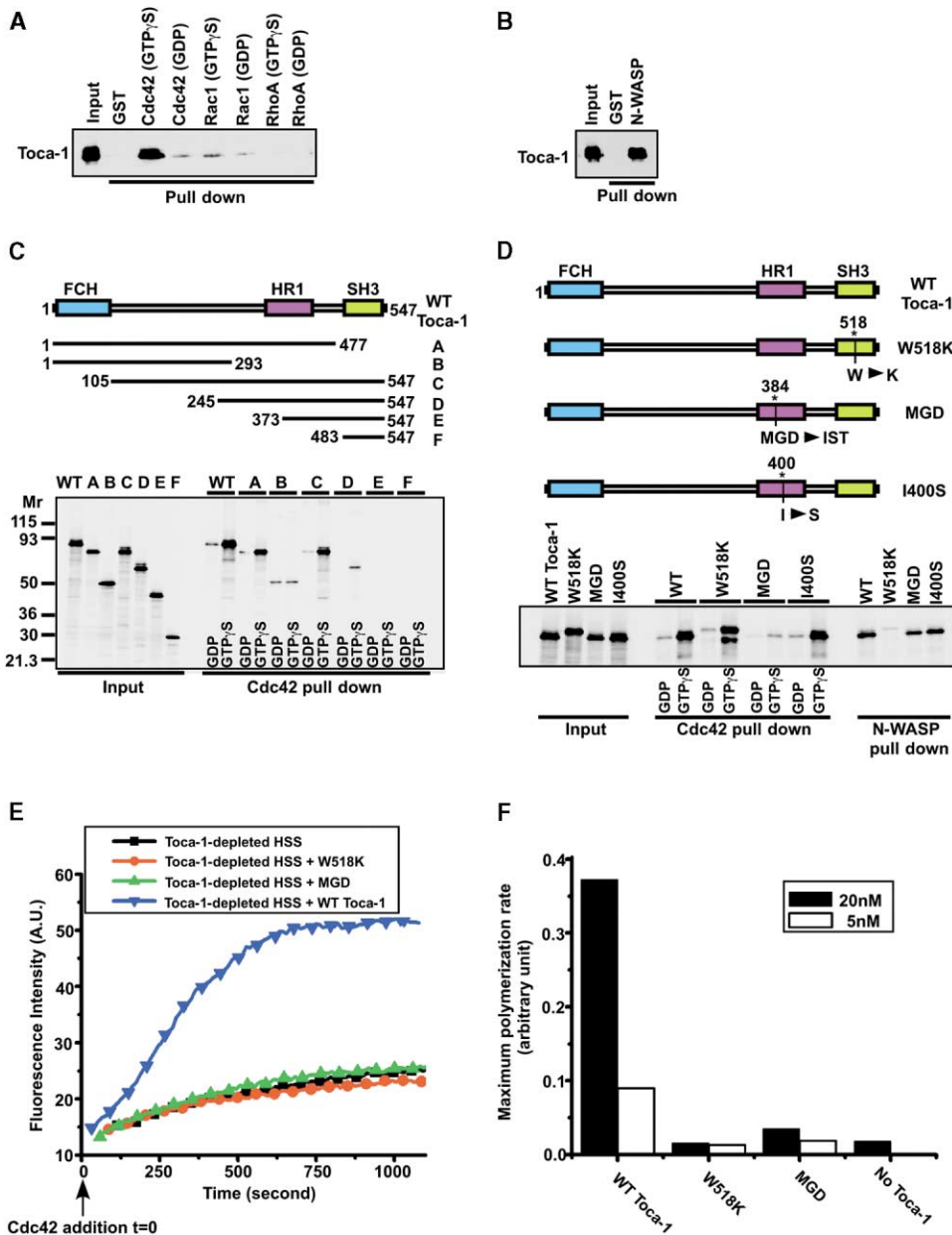
Figure 4. Direct Binding of Toca-1 to Cdc42 and N-WASP Is Required for Its Function

(A) Toca-1 directly interacts with Cdc42 in a GTP-dependent manner. GST-Cdc42, GST-Rac1, and GST-RhoA loaded with GTPγS or GDP were immobilized on glutathione-Sepharose beads and tested for their ability to bind purified recombinant Toca-1. Three percent of the input and 30% of the pulled down material were analyzed by α-Toca-1 immunoblotting. (B) Toca-1 directly interacts with N-WASP. The ability of GST-N-WASP to interact with Toca-1 was tested in the same type of pull-down assay as in (A). Five percent of the input and 5% of the pulled down material were analyzed by α-N-WASP immunoblotting. (C) (Top) A summary of the nomenclature and amino acid boundaries of the various human Toca-1 fragments used to map the Cdc42 binding site. (Bottom) The indicated protein constructs were synthesized as Myc-tagged, ^{35}S-labeled proteins by in vitro translation and tested for their abilities to bind specifically to GST-Cdc42-GTPγS immobilized on beads. Two percent of the input and 30% of the pulled down material were analyzed by SDS-PAGE and autoradiography. (D) (Top) Schematic diagram of the MGD to IST, the W518K, and the I400S mutants of human Toca-1 showing the sites of the mutations. The MGD, W518, and I400 residues are shown (boxed) in Figures 2A and 2D. (Bottom) The MGD, W518K, and I400S mutants were synthesized as ^{35}S-labeled proteins by in vitro translation and tested for their abilities to bind specifically to GST-Cdc42-GTPγS and to GST-N-WASP. Wild-type Toca-1 was used as the positive control. Two percent of the input and 30% (Cdc42 binding reactions) or 2% (N-WASP binding reactions) of the pulled down material were analyzed. The W518K doublet in the Cdc42 pull-down is likely due to partial proteolysis that occurred during the binding experiment (the level of the lower band is not reproducible). (E) Wild-type Toca-1, the MGD, and W518K mutants (5 nM each) were tested for their abilities to restore Cdc42-induced actin assembly in Toca-1-depleted Xenopus HSS. (F) Comparison of the abilities of wild-type Toca-1, the MGD, and the W518K mutants at 5 nM or 20 nM to rescue actin polymerization in Toca-1-depleted Xenopus HSS. Curves of the type shown in (E) are quantitated by measuring the maximum polymerization rate.

(Figures 2C and 2D). The functional conservation of Toca-1 across species is highlighted by the finding that Toca-1 homologs from *X. tropicalis* and *D. melanogaster* can complement the MCAP2B activity in our assay system (data not shown).

Toca-1 Is Essential for Cdc42- and PIP$_2$-Induced Actin Polymerization

We returned to the complete *Xenopus* extract system for biochemical analysis of Toca-1 in the Cdc42 pathway. In this system, the kinetics of actin polymerization can be monitored quantitatively using pyrene-labeled actin, a fluorescent derivative of actin that exhibits a dramatic increase in fluorescence intensity upon polymerization (Ma et al., 1998a). Using an affinity-purified α-Toca-1 polyclonal antibody, we immunodepleted >95% of endogenous Toca-1 from *Xenopus* HSS (Figure 3A). Cdc42-induced actin polymerization was drastically reduced in Toca-1-depleted HSS (Figure 3C). Importantly, the activity could be rescued by adding back purified recombinant Toca-1 at 5 nM (Figures 3B and 3C). Increasing the amount of Toca-1 resulted in a dose-dependent and saturable increase in the maximum polymerization rate. The concentration versus polymerization data was well fit by a hyperbolic binding isotherm that assumes a single binding site (Figure 3D). The concentration of Toca-1 required for half-maximal activation (K_{act}) is 14 nM, and the maximal polymerization rate at saturation (P_{max}) is 0.33/s. Comparing this P_{max} value to the polymerization rate in untreated extracts (0.082/s) suggests that Toca-1 is present at a concentration (∼5 nM) significantly lower than the K_{act}. This result agrees with the Toca-1 concentration determined by quantitative immunoblotting in these extracts (Toca-1, ∼10 nM; N-WASP, ∼100 nM). We confirmed that immunodepletion of Toca-1 from *Xenopus* HSS had no effect on the endogenous levels of N-WASP and the Arp2/3 complex, suggesting that the effect of Toca-1 depletion was specific (data not shown).

Toca-1 is also required for PIP$_2$-induced actin assembly. Synthetic lipid vesicles containing PIP$_2$ induce actin polymerization in *Xenopus* HSS, and this activity depends on the Cdc42-N-WASP-Arp2/3 pathway (Ma et al., 1998a; Rohatgi et al., 1999). PIP$_2$-induced actin assembly is eliminated in *Xenopus* HSS immunodepleted of Toca-1, and the activity can be rescued by adding back 10 nM recombinant Toca-1 protein (Figure 3E). Thus, Toca-1 is required for both Cdc42- and PIP$_2$-induced actin polymerization.

Direct Binding of Toca-1 to Cdc42 and N-WASP Is Required for Its Function

We expected that Toca-1 would directly bind to Cdc42-GTP, because the MCAP2B activity from brain HSS can be depleted with Cdc42-GTPγS-coated beads and because CIP4, a protein related to Toca-1, is a known Cdc42 binding protein (Aspenstrom, 1997). When recombinant Toca-1 was incubated with Cdc42-GTPγS or Cdc42-GDP immobilized on beads, it bound specifically to Cdc42-GTPγS (Figure 4A). No specific interaction was detected between Toca-1 and Rac1 or RhoA under the same conditions. Purified Toca-1 directly interacts with N-WASP as well (Figure 4B), consistent with a previously

reported interaction between the SH3 domain of CIP4 and WASP (Tian et al., 2000).

To map the region of Toca-1 required for binding to Cdc42, Toca-1 fragments were tested for their ability to selectively interact with Cdc42-GTPγS (Figure 4C). This deletion analysis identified the region between amino acids 245 and 477, a region that contains the HR1 domain, as minimally essential for Cdc42 binding. The region between amino acids 105 and 244 contributes to the efficiency of this interaction, perhaps by promoting the proper folding of Toca-1. These regions overlap with the previously mapped Cdc42 binding site in CIP4 (CIP4 amino acid residues 383–417, corresponding to residues 385–417 in Toca-1) (Tian et al., 2000). Although the HR1 domain was not yet clearly defined and thus not recognized in CIP4 and FBP17 at the times these proteins were first described, it is now clear that both CIP4 and FBP17 also contain HR1 domains (see Figures 2C and 2D). The HR1 domain was originally implicated in the interactions of several RhoA binding proteins, including PRK1/PKN, rhotekin, rhophilin, and p160ROCK, with RhoA (Flynn et al., 1998). Interestingly, whereas the first HR1 (HR1a) domain from the regulatory N-terminal region of PRK1 interacts specifically with RhoA, the second HR1 (HR1b) from the same protein has been shown recently to interact specifically with Rac1 (Flynn et al., 1998; Owen et al., 2003). Both HR1a and HR1b domains from PRK1 adopt an antiparallel coiled-coil finger fold, which makes direct contacts with RhoA or Rac1 (Maesaki et al., 1999; Owen et al., 2003).

Our results clearly define a new class of HR1 domains, including those found in Toca-1, CIP4, and likely FBP17, that mediates specific interactions with Cdc42 (Figures 2D and 4A). Secondary structure modeling of the Toca-1 HR1 domain suggests that its structure is very similar to those described for the PRK1 HR1s (Maesaki et al., 1999; Owen et al., 2003). Thus, the HR1 antiparallel coiled-coil finger structure appears to be a general scaffold for interactions with Rho-family GTPases, and amino acid differences between the HR1 domains likely determine specificity for different Rho GTPases (Figure 2D). In addition to its presence in several PCH family proteins, the HR1 domain can be found in a large number of other proteins in GenBank. Thus, HR1 domains should be thought of as a new class of small G protein binding domains (such as the CRIB domain) that define a group of proteins linked to small GTPase signaling.

To test the functional significance of Toca-1's interactions with Cdc42 and N-WASP, we generated Toca-1 mutants defective in these activities. As shown in Figure 4D, the MGD mutant, with three conserved residues (MGD) in the HR1 domain substituted with IST, is significantly impaired in its ability to bind Cdc42 (but not N-WASP). Notably, the I398S mutation in CIP4 has been shown to abrogate binding to Cdc42 (Tian et al., 2000); however, the analogous mutant of Toca-1 (I400S) is unaffected (Figure 4D). The W518K mutant, with a conserved tryptophan in the SH3 domain mutated to a lysine, no longer binds to N-WASP but can still bind Cdc42 with high affinity (Figure 4D).

The MGD (HR1) and W518K (SH3) mutants were tested for their ability to restore Cdc42-induced actin assembly in extracts depleted of endogenous Toca-1. While wild-type Toca-1 at 5 nM effectively rescued actin polymer-
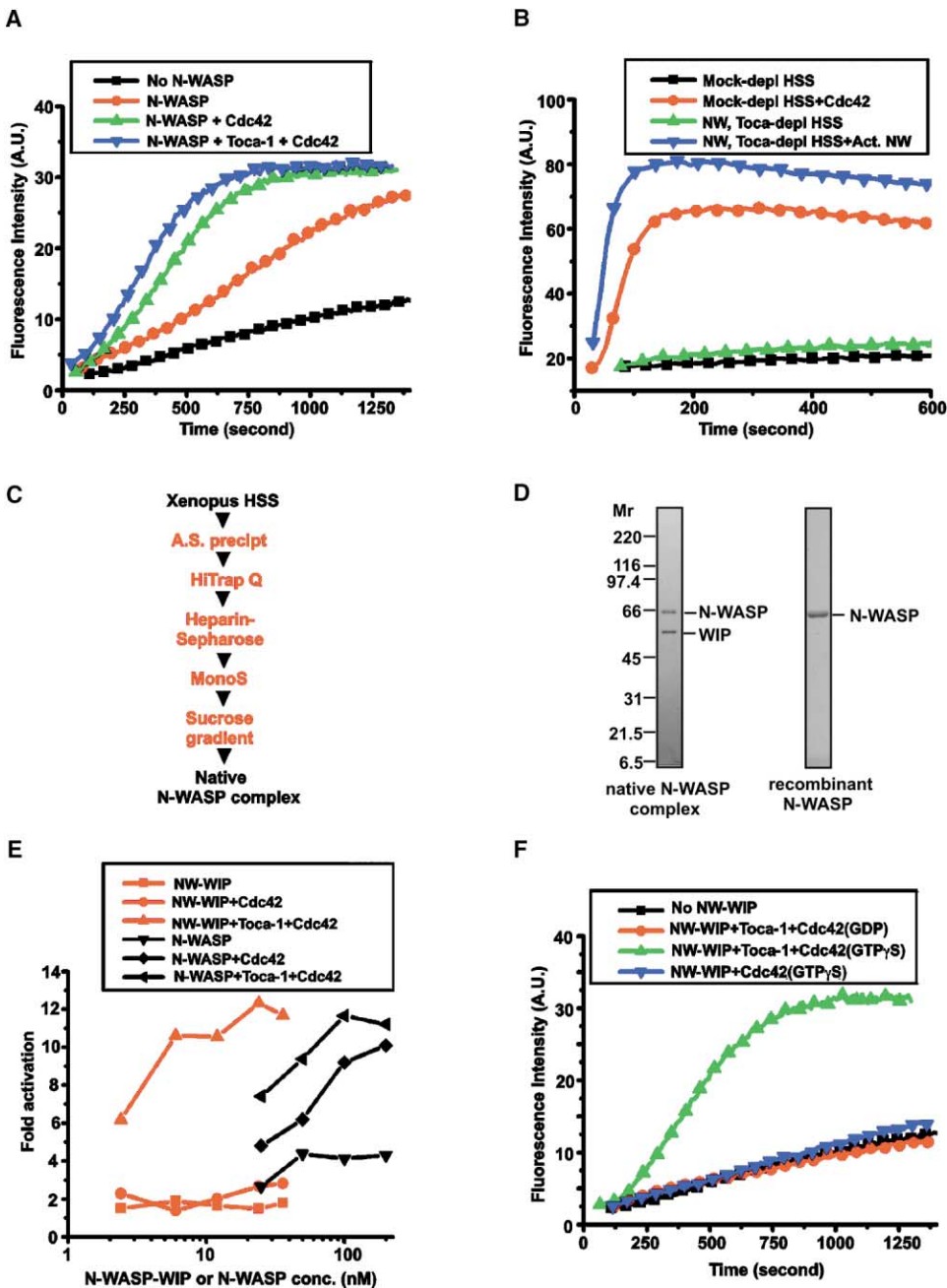
Figure 5. Toca-1 Is Required for Cdc42-Dependent Activation of the Native N-WASP-WIP Complex

(A) The pyrene-actin assay was used to compare the effect of Toca-1 (10 nM) on actin polymerization (2 μM total G-actin; 35% pyrene labeled) in the presence of Arp2/3 complex (30 nM), recombinant N-WASP (100 nM), and Cdc42-GTPγS (250 nM). All reactions contain actin and the Arp2/3 complex, and the other factors are present as indicated.

(B) A constitutively active N-WASP mutant (Act. NW) can induce actin polymerization in Xenopus HSS depleted of both endogenous N-WASP and Toca-1. The polymerization kinetics in mock-depleted HSS with or without Cdc42-GTPγS stimulation are shown as controls.

(C) The fractionation scheme used to purify the native N-WASP-WIP complex from Xenopus egg HSS. During the purification, the complex was followed by α-N-WASP immunoblotting.

(D) Purified preparations of native N-WASP-WIP complex and recombinant untagged N-WASP used in the actin polymerization experiments shown in (A), (E), and (F) are shown on a 4%–20% SDS-polyacrylamide gel. Xenopus WIP copurified with N-WASP as a stoichiometric complex and was identified by mass spectrometry.

(E) The pyrene-actin assay was used to compare the activation of recombinant free N-WASP to that of the purified native N-WASP-WIP complex at several different concentrations by Cdc42-GTPγS (250 nM) alone or Cdc42-GTPγS (250 nM) + Toca-1 (10 nM). All reactions contained 2 μM G actin (35% pyrene labeled) and 30 nM Arp2/3 complex. The fold increase (above a background reaction lacking any N-WASP) in the maximum polymerization rate is plotted as a function of N-WASP and N-WASP-WIP concentrations.

(F) The pyrene-actin assay was used to compare the activation of the purified N-WASP-WIP complex (6 nM) by Cdc42-GTPγS (250 nM) in the presence or absence of Toca-1 (10 nM). Cdc42-GDP (250 nM) is completely inactive in inducing actin polymerization in the presence of both the N-WASP-WIP complex and Toca-1. All reactions contained 2 μM G actin (35% pyrene labeled) and 30 nM Arp2/3 complex.

ization in these extracts, the MGD (HR1) and the W518K (SH3) mutants were both completely inactive at this concentration (Figures 4E and 4F). At 20 nM, the MGD mutant exhibited a slight activity ($\sim$15% of wild-type at the same concentration) (Figure 4F), likely reflecting its residual affinity for Cdc42 (Figure 4D). The W518K mutant was still completely inactive at 20 nM (Figure 4F). In summary, the ability of Toca-1 to interact with both Cdc42 and N-WASP is required for its function. Since SH3 domains display promiscuous interactions with proline-rich proteins (such as N-WASP) under purified conditions, we cannot exclude the possibility that the SH3 domain of Toca-1 interacts with proteins other than N-WASP in extracts.

Toca-1 Is Required for Cdc42 to Activate the Native N-WASP-WIP Complex
Thus far, we have established the requirement of Toca-1 for Cdc42- and PIP$_2$-induced actin nucleation in cell extracts. Surprisingly, when we added Toca-1 to the purified system, consisting of Cdc42-GTPγS, recombinant N-WASP, and the Arp2/3 complex, there was only a small effect on the actin polymerization kinetics (Figure 5A). Again, this confirms the initial observation that led us to pursue the purification of Toca-1—the Cdc42 pathway in extracts is significantly different from the purified system. There are two possible explanations for this difference in the requirement for Toca-1 between these systems. First, N-WASP activity in extracts might be subject to an additional level of inhibition not present in the purified system, and Toca-1 is involved in relieving this inhibition. Alternatively, the extracts contain an inhibitor of actin polymerization, such as a filament-capping activity (Huang et al., 1999) not present in the purified system, and Toca-1 is required to antagonize such an inhibitor.

If the requirement of Toca-1 were at the level of N-WASP activation, this requirement would be bypassed by replacing endogenous N-WASP with a constitutively active form of N-WASP. However, if Toca-1 antagonizes an inhibitor of actin polymerization, it should still be required for actin polymerization induced by the constitutively active N-WASP. Consistent with the former prediction, Toca-1 is no longer required for actin polymerization when endogenous N-WASP in extract is replaced with a constitutively active mutant of N-WASP (Figure 5B; see Supplemental Data on *Cell* web site for a complete description and characterization of the constitutively active N-WASP mutant). We have previously found that native N-WASP exists in a tight complex with CR16 in bovine brain (Ho et al., 2001). A similar complex between WASP and WIP, a protein closely related to CR16, has also been reported (Ramesh et al., 1997). Importantly, WIP can suppress the activation of recombinant N-WASP by Cdc42 in vitro (Martinez-Quiles et al., 2001). Thus, we speculated that the requirement for Toca-1 in extracts might reflect its ability to activate the endogenous N-WASP-WIP/CR16 complex, a requirement that is not present in the purified system since it uses recombinant N-WASP not bound to WIP/CR16.

WIP and CR16 have unusually high ($\sim$30%) proline contents and are difficult to express as soluble recombinant proteins that are fully functional in our assay system, even

as a complex with N-WASP (data not shown). Therefore, we conventionally purified the native N-WASP-WIP complex from *Xenopus* eggs (Figures 5C and 5D). Using an in vitro purified system consisting of the native N-WASP-WIP complex from *Xenopus* eggs or recombinant N-WASP from SF9 cells, Cdc42-GTPγS, and the Arp2/3 complex, the behavior of the N-WASP-WIP complex was directly compared to that of recombinant free N-WASP over a wide range of concentrations (Figure 5E). Again, Toca-1 had only a small stimulatory effect on the activation of recombinant free N-WASP by Cdc42-GTPγS (Figure 5E). In contrast, activation of the native N-WASP-WIP complex by Cdc42-GTPγS strongly depended on the presence of Toca-1 (Figures 5E and 5F). Furthermore, while recombinant free N-WASP exhibits significant basal activity even in the absence of Cdc42, the N-WASP-WIP complex displays virtually no basal activity and absolutely depends on the presence of both Cdc42 and Toca-1 for activation (Figures 5E and 5F). Noticeably, the native N-WASP-WIP complex has a specific activity approximately one order of magnitude higher than that of recombinant N-WASP (Figure 5E). We conclude that Toca-1 is required for Cdc42-GTP to activate the N-WASP-WIP/CR16 complex, the predominant form of N-WASP in cells. This provides a mechanistic explanation for the requirement of Toca-1 in mediating Cdc42-induced actin polymerization in extracts.

Toca-1 Is Required for PMA-Induced Actin Comet Formation and Vesicle Motility in *Xenopus* Extracts
Work in many systems has suggested that N-WASP- and Arp2/3-dependent actin nucleation is directly linked to membrane trafficking (Schafer, 2002; Sokac et al., 2003). Actin comet tails, similar to those assembled by *Listeria*, *Shigella*, and *Vaccinia* virus, have been shown to power the intracellular motility of pinosomes, lysosomes, and endosomes in a variety of cell types (Allen, 2003; Kaksonen et al., 2003; Merrifield et al., 1999; Rozelle et al., 2000). The propulsive movement of endocytic vesicles by actin comets has also been observed in whole *Xenopus* eggs and shown to be triggered by a protein kinase C (PKC)-mediated signaling cascade in vivo (Taunton et al., 2000). This process has been reconstituted in a cell-free system in *Xenopus* egg extracts stimulated with the PKC activator PMA and depends on Cdc42, N-WASP, and the Arp2/3 complex (Taunton et al., 2000).

Since Toca-1 is an essential component of the Cdc42 pathway, we tested whether Toca-1 is also required for actin comet-based vesicle motility using this assay. As previously reported, PMA can stimulate the assembly of actin comet tails on vesicle surfaces in *Xenopus* HSS supplemented with endomembranes isolated from HeLa cells (Figure 6A). PMA-induced actin comet formation in these extracts was abolished by antibody depletion of Toca-1 (Figure 6A). The α-Toca-1 antibody (30 nM) was maintained in the reaction to neutralize the Toca-1 activity carried over from HeLa lysates. Addback of recombinant Toca-1 at 150 nM completely rescued actin comet tail formation. Higher concentrations of Toca-1 resulted in the formation of longer actin comet tails, presumably due to an increased rate of actin nucleation
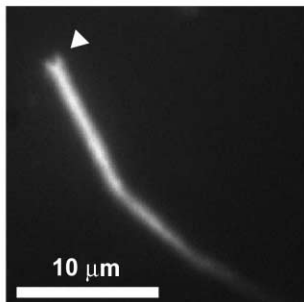
A
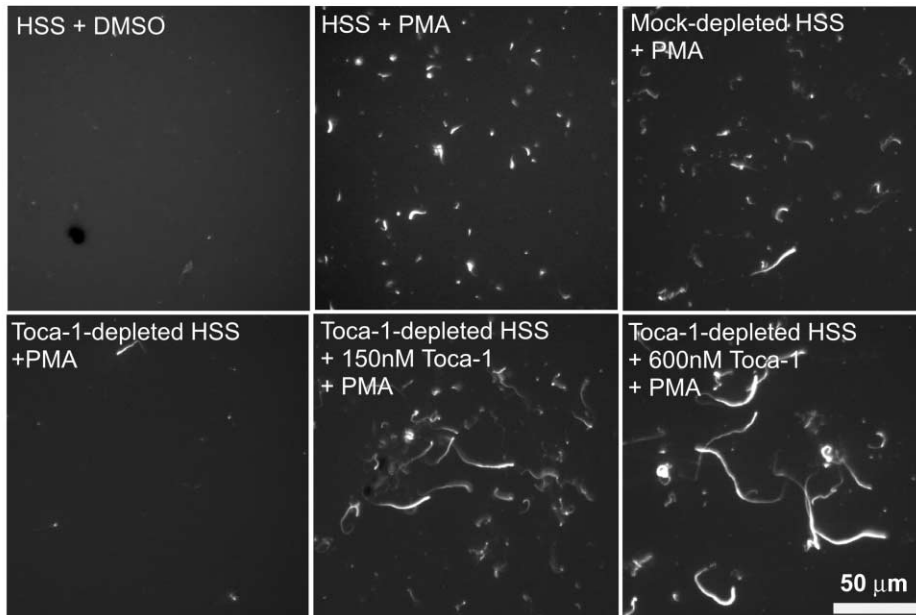
B

Figure 6. Toca-1 Is Required for PMA-Induced Actin Comet Tail Assembly on the Surface of Intracellular Vesicles

(A) Comparison of PMA-induced actin comet tail formation on the surface of HeLa endomembrane vesicles in *Xenopus* HSS, mock-depleted HSS, Toca-1-depleted HSS, Toca-1-depleted HSS rescued with 150 nM Toca-1, and Toca-1-depleted HSS rescued with 600 nM Toca-1. Note that the α-Toca-1 antibody (30 nM) was maintained in the Toca-1-depleted HSS to neutralize the Toca-1 activity carried over from HeLa lysates. DMSO was used as the negative control for PMA stimulation.
(B) A high-magnification view of a comet tail emanating from a vesicle surface (arrowhead).

and a constant rate of filament disassembly (Figure 6A). As previously reported (Taunton et al., 2000), PMA-induced comets were associated with membrane vesicles, suggesting actin is nucleated on vesicle surfaces (Figure 6B).

Discussion

A Revised View of Cdc42 Signaling to the Actin Cytoskeleton

In this paper, we have demonstrated that the previously identified components of the Cdc42-signaling pathway, namely N-WASP and the Arp2/3 complex, are not sufficient to mediate actin assembly in a physiological context. Instead, the PCH family protein Toca-1 is required to activate the N-WASP-WIP complex present in cell extracts. In this revised model, activated Cdc42 inter-

acts with both Toca-1 and the N-WASP-WIP complex, and these interactions lead to the activation of N-WASP, which in turn stimulates actin nucleation through the Arp2/3 complex (Figure 7).

A special feature of this Cdc42-dependent signaling network is the control of actin nucleation by coupling two Cdc42-dependent regulatory branches (Figure 7), mediated by the Cdc42-N-WASP and Cdc42-Toca-1 interactions. This arrangement allows for increased fidelity as well as regulatory flexibility in this pathway. For instance, since Cdc42 is coupled to several other pathways in the cell, Toca-1, present at concentrations well below saturation (Figure 3D), is ideally suited to regulate flux down the Cdc42-N-WASP-Arp2/3 pathway. We expect to find other signaling pathways that directly modulate the activity of Toca-1.

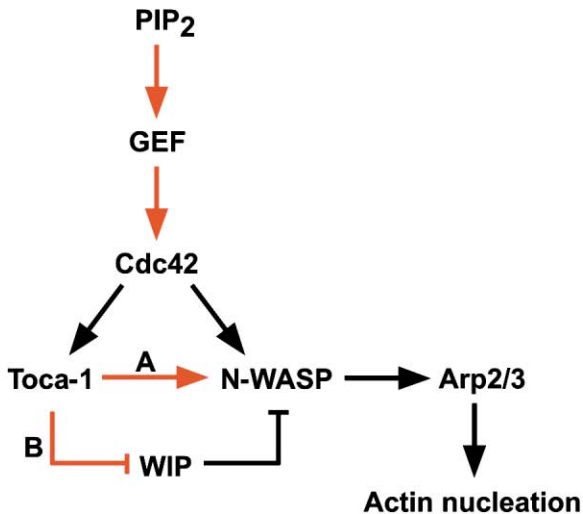An intriguing question raised by our data is whether

Figure 7. Model for the Regulation of Actin Nucleation by Cdc42

See Discussion for details. Black arrows indicate confirmed functional interactions. Red arrows indicate speculative interactions. Toca-1 can either directly activate N-WASP (A) or indirectly activate N-WASP by inhibiting WIP (B). GEF, guanine nucleotide exchange factor.

Cdc42 can bind both N-WASP and Toca-1 simultaneously. Though we have found that a CRIB-containing fragment of N-WASP does not compete with Toca-1 for binding to Cdc42 (data not shown), additional analyses are needed to elucidate the precise physical arrangement of the Cdc42-Toca-1 and Cdc42-N-WASP interactions.

This work reveals an important biochemical function for a PCH family member, namely the stimulation of actin nucleation. Our finding that Toca-1 is required for both Cdc42 and N-WASP-dependent actin nucleation and the actin comet-based propulsive movement of endomembrane vesicles provides a functional link between actin assembly and membrane trafficking (Schafer, 2002). More generally, PCH family proteins may serve to link various cellular processes to actin nucleation mediated by WASP family members.

The Role of PIP$_2$ in Cdc42-Dependent Actin Assembly

We have previously suggested two roles for PIP$_2$ in the Cdc42 pathway: one at the level of N-WASP activation and the second at a more upstream point at the level of Cdc42 activation through a guanine nucleotide exchange factor. These conclusions are based on two observations: PIP$_2$ can bind and activate N-WASP in cooperation with Cdc42; however, a mutant of N-WASP that cannot bind or respond to PIP$_2$ in vitro can largely restore PIP$_2$-induced actin assembly to N-WASP-depleted extracts (Rohatgi et al., 2000). The latter observation suggests that the major function of PIP$_2$ in extracts is not directly at the level of N-WASP activation but rather at a more upstream step. An important question raised by this work is whether PIP$_2$ and Toca-1 are redundant activators of N-WASP. In fact, the N-WASP-WIP complex can be fully activated by Cdc42 and PIP$_2$ just as it can by

Toca-1 and Cdc42 (Ho et al., 2001). However, Toca-1 and PIP$_2$ are not redundant in the more physiological milieu of extracts, because Toca-1 immunodepletion abrogates PIP$_2$-induced actin assembly. This finding suggests that the major role of PIP$_2$ in extracts is upstream of N-WASP, perhaps at the level of Cdc42 activation (Figure 7).

Functional Significance of the N-WASP-WIP Interaction: Insight into the Molecular Pathogenesis of Wiskott-Aldrich Syndrome

Direct comparison of purified native N-WASP-WIP complex and recombinant free N-WASP in the actin polymerization assay suggests that WIP can suppress not only the activation of N-WASP by Cdc42 alone but also the basal activation of N-WASP in the absence of any activators (Figures 5E and 5F), consistent with previous findings (Martinez-Quiles et al., 2001). It is probably physiologically important for WIP to suppress the activity of N-WASP. Without WIP, a small but significant amount of N-WASP likely populates the active state, since recombinant N-WASP exhibits basal Arp2/3-activating activity even without activators like Cdc42 (Figures 5A and 5E). This unregulated stimulation of actin assembly would be dangerous to the cell. We propose that WIP functions by stabilizing the autoinhibited conformation of N-WASP in the absence of genuine activating signals. Alternatively, posttranslational modification of the N-WASP-WIP complex or additional substoichiometric factors present in the N-WASP-WIP preparation could also potentially contribute to the regulation of this complex by Toca-1.

We envision two possible mechanisms by which Toca-1 can regulate the N-WASP-WIP complex. First, Toca-1 could directly activate N-WASP by destabilizing the inhibitory intramolecular interaction. Alternatively, Toca-1 could indirectly contribute to N-WASP activation by antagonizing the suppressive activity of WIP. In the latter case, the simultaneous activation and derepression of N-WASP, both through Cdc42, would generate a sharp temporal transition between the inactive and the active states of N-WASP. In addition, the requirement for two or possibly more Cdc42 interactions (Cdc42-N-WASP and Cdc42-Toca-1) in this pathway would permit a spatially synergistic response at sites of local Cdc42 activation. We await a more quantitative examination of the pathway to test these possibilities.

An important question concerning the regulation of the N-WASP-WIP complex is whether binding of Toca-1 to the complex (either through N-WASP or WIP or both) leads to the dissociation of the complex. Due to the inability to produce functional free WIP, we have not been able to test the possible interaction between WIP and Toca-1. Consequently, even though Toca-1 coated beads, when mixed with the native N-WASP-WIP complex, can pull down both N-WASP and WIP (data not shown), it is not clear whether these proteins are bound to Toca-1 beads as an intact complex or as dissociated subunits.

Our model may have important implications for understanding the mechanism of the pediatric disease Wiskott-Aldrich syndrome (WAS). WAS is an X-linked recessive disorder characterized by thrombocytopenia,

eczema, and immunodeficiency, all phenotypes that have been linked to misregulation of the actin cytoskeleton (Snapper and Rosen, 2003). A majority (28/35) of disease-causing missense mutations in WASP are predicted to disrupt the WASP-WIP interactions, based on a recently solved NMR structure of the interface (Volkman et al., 2002). Thus, one important outstanding question in this disease is understanding the consequence of disrupting the WASP-WIP interaction. Our results provide a possible answer to this question—disruption of the WASP-WIP interaction would eliminate the Toca-1 input into this pathway and prevent appropriate temporal and spatial regulation of actin assembly in response to Cdc42 signals. In fact, lymphocytes from WIP knockout mice have severe deficits in signal-induced changes in their cortical actin cytoskeleton (Anton et al., 2002).

In summary, we propose the following view of the Cdc42 signaling pathway (Figure 7). Formation of PIP_2 on membranes (such as a vesicle surface) leads to the recruitment and activation of Cdc42. Prenylated Cdc42 inserts into the membrane and forms high avidity sites that recruit Toca-1 and the N-WASP-WIP complex. Activation of N-WASP then could proceed through one of two paths: both Cdc42 and Toca-1 could cooperate to activate the N-WASP-WIP complex, or Toca-1 could function indirectly by relieving the inhibition of N-WASP by WIP. Toca-1 is ideally positioned to be an important regulatory node for the Cdc42 pathway. The function of Toca-1 suggests a specific mechanism by which PCH family proteins can influence actin nucleation in a wide variety of cellular processes such as vesicle motility and cytokinesis. Important future questions include the precise biochemical mechanism by which the N-WASP-WIP complex is activated by Toca-1 and Cdc42, as well as investigation into the regulation of Toca-1 itself by other signals.

Experimental Procedures

Conventional Protein Fractionation
Bovine brain Toca-1, Arp2/3 complex, and *Xenopus* N-WASP-WIP complex were purified using conventional protein fractionation techniques. Experimental details are described in Supplemental Data.

Protein Identification by Tandem Mass Spectrometry
Protein identification by tandem mass spectrometry was performed as described (Gygi et al., 1999).

Actin Polymerization Assays
Rhodamine-actin microscopic assays using bovine brain extracts were performed as previously described for *Xenopus* HSS (Ma et al., 1998b).

Pyrene-actin was used to follow actin polymerization in *Xenopus* extracts as described previously (Ma et al., 1998b). Polymerization was initiated by addition of 250 nM GST-Cdc42-GTPγS or 10 μM lipid vesicles containing 10% PI(4,5)P_2, 45% phosphatidylcholine, and 45% phosphatidylinositol.

Actin polymerization assays using purified components were performed as previously described (Rohatgi et al., 1999). All reactions contained 2 μM purified rabbit muscle actin (35% pyrene labeled), 30 nM purified bovine Arp2/3 complex, 250 nM purified prenylated GST-Cdc42 produced in insect cells, and indicated concentrations of Toca-1, N-WASP, or the N-WASP-WIP complex.

Molecular Biology
Cloning of human Toca-1 cDNA is described in Supplemental Data. The cDNA encoding *Xenopus tropicalis* Toca-1 was isolated from an expressed sequence tag (EST) clone (GenBank accession number AL655809) by PCR. Mutagenesis was performed by PCR or by using the GeneEditor Mutagenesis Kit (Promega). All constructs were confirmed by sequencing.

For in vitro translation, full-length or fragments of Toca-1 were cloned into the pCS2+ or pCS2+MT vectors. For baculoviral construction, Toca-1 was cloned into the pFastBacHT vector, which contains a hexahistidine tag located N-terminal to the cloning sites.

Preparation of Recombinant Proteins
GST-Cdc42, GST-Rac1, and GST-RhoA were prepared from Sf9 cells and loaded with different nucleotides (GTPγS or GDP) while still bound to glutathione-Sepharose beads according to established protocols (Ma et al., 1998a).

Hexahistidine-tagged wild-type or mutant Toca-1 proteins were expressed in SF9 cells and affinity purified on nickel-Sepharose beads. Proteins were eluted in 50 mM Na-phosphate (pH 7.8), 400 mM NaCl, 260 mM imidazole, 5 mM β-ME.

Untagged rat N-WASP expressed in SF9 cells was purified as previously described (Rohatgi et al., 1999).

Protein concentrations were determined by the Bradford assay (Bio-Rad) or by densitometry of GelCode Blue (Pierce) stained gels, using BSA as a standard in both cases.

In vitro translations were performed using the Promega TNT kit and ^{35}S-methionine according to manufacturer's instructions.

Preparation of Antibodies
Purified full-length human Toca-1 was used to raise antisera in rabbits (Cocalico, Reamstown, PA). The antibodies were affinity purified according to established protocols (Harlow and Lane, 1999).

Immunodepletion
Affinity-purified α-Toca-1 or nonspecific rabbit IgG (7 μg) was first incubated with 25 μL Protein A-Dynabeads (Dynal) in PBS plus 0.1% Triton X-100. Beads were washed twice with PBS plus 0.1% Triton X-100 and three times with XB (*Xenopus* extract buffer, 30 mM HEPES [pH 7.7], 100 mM KCl, 1 mM MgCl₂). *Xenopus* HSS (100 μL) were incubated with antibody-coated beads and rotated at 4°C for 1.5 hr. Beads were removed by centrifugation, and the supernatants were used for actin polymerization within 6 hr.

Protein Binding Assays
For GST pull-down assays using purified recombinant Toca-1, 8 μg of GST-tagged protein (Cdc42, Rac1, RhoA, or N-WASP) immobilized on 8 μL glutathione-Sepharose was incubated at 4°C with 0.5 μg of purified human Toca-1 in 50 μL of XB containing 1 mg/ml of chicken egg albumin. The beads were washed once with XB plus 0.25% Triton X-100, once with XB plus 200mM KCl and 0.1% Triton X-100, and once with XB plus 0.1% Triton X-100. Proteins bound to the beads were eluted with SDS sample buffer and analyzed by immunoblotting.

GST pull-down assays using ^{35}S-labeled proteins were performed as described above. The reticulocyte lysate (10 μL) containing the ^{35}S-labeled proteins were used in each binding reaction. The labeled proteins were visualized using a PhosphorImager (Bio-Rad).

PMA-Induced Vesicle Motility Assays
PMA-induced vesicle motility assays were performed as described (Taunton et al., 2000). Actin comet tails were induced by addition of PMA (2 μM final) to *Xenopus* HSS supplemented with HeLa postnuclear supernatant containing endomembranes. HSS was immunodepleted with α-Toca-1 or nonspecific IgG. An additional 30 nM of the respective antibodies was added to the final reactions to neutralize Toca-1 carried over from the HeLa cell endomembranes.

Data Analysis
All kinetic analyses were performed using Origin (Microcal Software). Maximum elongation rates from pyrene-actin polymerization reactions were calculated from the slopes of the linear, elongation phase of the actin assembly curves. All data shown in the figures were taken from experiments performed at least twice. Toca-1 dose-response data were fitted by least squares nonlinear regression

using GraphPad Prism 4. Protein sequence analyses were performed using ScanSite and Clustal W.

References

Allen, P.G. (2003). Actin filament uncapping localizes to ruffling lamellae and rocketing vesicles. Nat. Cell Biol. *5*, 972–979.

Anton, I.M., de la Fuente, M.A., Sims, T.N., Freeman, S., Ramesh, N., Hartwig, J.H., Dustin, M.L., and Geha, R.S. (2002). WIP deficiency reveals a differential role for WIP and the actin cytoskeleton in T and B cell activation. Immunity *16*, 193–204.

Aspenstrom, P. (1997). A Cdc42 target protein with homology to the non-kinase domain of FER has a potential role in regulating the actin cytoskeleton. Curr. Biol. *7*, 479–487.

Carlier, M.F., Nioche, P., Broutin-L'Hermite, I., Boujemaa, R., Le Clainche, C., Egile, C., Garbay, C., Ducruix, A., Sansonetti, P., and Pantaloni, D. (2000). GRB2 links signaling to actin assembly by enhancing interaction of neural Wiskott-Aldrich syndrome protein (N-WASp) with actin-related protein (ARP2/3) complex. J. Biol. Chem. *275*, 21946–21952.

Cory, G.O., Cramer, R., Blanchoin, L., and Ridley, A.J. (2003). Phosphorylation of the WASP-VCA domain increases its affinity for the Arp2/3 complex and enhances actin polymerization by WASP. Mol. Cell *11*, 1229–1239.

Derry, J.M., Ochs, H.D., and Francke, U. (1994). Isolation of a novel gene mutated in Wiskott-Aldrich syndrome. Cell *78*, 635–644.

Etienne-Manneville, S., and Hall, A. (2002). Rho GTPases in cell biology. Nature *420*, 629–635.

Flynn, P., Mellor, H., Palmer, R., Panayotou, G., and Parker, P.J. (1998). Multiple interactions of PRK1 with RhoA. Functional assignment of the Hr1 repeat motif. J. Biol. Chem. *273*, 2698–2705.

Gygi, S.P., Han, D.K., Gingras, A.C., Sonenberg, N., and Aebersold, R. (1999). Protein analysis by mass spectrometry and sequence database searching: tools for cancer research in the post-genomic era. Electrophoresis *20*, 310–319.

Harlow, E., and Lane, D. (1999). Using Antibodies: A Laboratory Manual (Cold Spring Harbor, NY: Cold Spring Harbor Laboratory Press).

Ho, H.Y., Rohatgi, R., Ma, L., and Kirschner, M.W. (2001). CR16 forms a complex with N-WASP in brain and is a novel member of a conserved proline-rich actin-binding protein family. Proc. Natl. Acad. Sci. USA *98*, 11306–11311.

Huang, M., Yang, C., Schafer, D.A., Cooper, J.A., Higgs, H.N., and Zigmond, S.H. (1999). Cdc42-induced actin filaments are protected from capping protein. Curr. Biol. *9*, 979–982.

Kaksonen, M., Sun, Y., and Drubin, D.G. (2003). A pathway for association of receptors, adaptors, and actin during endocytic internalization. Cell *115*, 475–487.

Kim, A.S., Kakalis, L.T., Abdul-Manan, N., Liu, G.A., and Rosen, M.K.

(2000). Autoinhibition and activation mechanisms of the Wiskott-Aldrich syndrome protein. Nature *404*, 151–158.

Lippincott, J., and Li, R. (2000). Involvement of PCH family proteins in cytokinesis and actin distribution. Microsc. Res. Tech. *49*, 168–172.

Ma, L., Cantley, L.C., Janmey, P.A., and Kirschner, M.W. (1998a). Corequirement of specific phosphoinositides and small GTP-binding protein Cdc42 in inducing actin assembly in Xenopus egg extracts. J. Cell Biol. *140*, 1125–1136.

Ma, L., Rohatgi, R., and Kirschner, M.W. (1998b). The Arp2/3 complex mediates actin polymerization induced by the small GTP-binding protein Cdc42. Proc. Natl. Acad. Sci. USA *95*, 15362–15367.

Machesky, L.M., Mullins, R.D., Higgs, H.N., Kaiser, D.A., Blanchoin, L., May, R.C., Hall, M.E., and Pollard, T.D. (1999). Scar, a WASp-related protein, activates nucleation of actin filaments by the Arp2/3 complex. Proc. Natl. Acad. Sci. USA *96*, 3739–3744.

Maesaki, R., Ihara, K., Shimizu, T., Kuroda, S., Kaibuchi, K., and Hakoshima, T. (1999). The structural basis of Rho effector recognition revealed by the crystal structure of human RhoA complexed with the effector domain of PKN/PRK1. Mol. Cell *4*, 793–803.

Martinez-Quiles, N., Rohatgi, R., Anton, I.M., Medina, M., Saville, S.P., Miki, H., Yamaguchi, H., Takenawa, T., Hartwig, J.H., Geha, R.S., and Ramesh, N. (2001). WIP regulates N-WASP-mediated actin polymerization and filopodium formation. Nat. Cell Biol. *3*, 484–491.

Merrifield, C.J., Moss, S.E., Ballestrem, C., Imhof, B.A., Giese, G., Wunderlich, I., and Almers, W. (1999). Endocytic vesicles move at the tips of actin tails in cultured mast cells. Nat. Cell Biol. *1*, 72–74.

Miki, H., Suetsugu, S., and Takenawa, T. (1998). WAVE, a novel WASP-family protein involved in actin reorganization induced by Rac. EMBO J. *17*, 6932–6941.

Owen, D., Lowe, P.N., Nietlispach, D., Brosnan, C.E., Chirgadze, D.Y., Parker, P.J., Blundell, T.L., and Mott, H.R. (2003). Molecular dissection of the interaction between the small G proteins Rac1 and RhoA and protein kinase C-related kinase 1 (PRK1). J. Biol. Chem. *278*, 50578–50587.

Ramesh, N., Anton, I.M., Hartwig, J.H., and Geha, R.S. (1997). WIP, a protein associated with Wiskott-Aldrich syndrome protein, induces actin polymerization and redistribution in lymphoid cells. Proc. Natl. Acad. Sci. USA *94*, 14671–14676.

Rohatgi, R., Ma, L., Miki, H., Lopez, M., Kirchhausen, T., Takenawa, T., and Kirschner, M.W. (1999). The interaction between N-WASP and the Arp2/3 complex links Cdc42-dependent signals to actin assembly. Cell *97*, 221–231.

Rohatgi, R., Ho, H.Y., and Kirschner, M.W. (2000). Mechanism of N-WASP activation by CDC42 and phosphatidylinositol 4,5-bisphosphate. J. Cell Biol. *150*, 1299–1310.

Rohatgi, R., Nollau, P., Ho, H.Y., Kirschner, M.W., and Mayer, B.J. (2001). Nck and phosphatidylinositol 4,5-bisphosphate synergistically activate actin polymerization through the N-WASP-Arp2/3 pathway. J. Biol. Chem. *276*, 26448–26452.

Rozelle, A.L., Machesky, L.M., Yamamoto, M., Driessens, M.H., Insall, R.H., Roth, M.G., Luby-Phelps, K., Marriott, G., Hall, A., and Yin, H.L. (2000). Phosphatidylinositol 4,5-bisphosphate induces actin-based movement of raft-enriched vesicles through WASP-Arp2/3. Curr. Biol. *10*, 311–320.

Schafer, D.A. (2002). Coupling actin dynamics and membrane dynamics during endocytosis. Curr. Opin. Cell Biol. *14*, 76–81.

Snapper, S.B., and Rosen, F.S. (2003). A family of WASPs. N. Engl. J. Med. *348*, 350–351.

Sokac, A.M., Co, C., Taunton, J., and Bement, W. (2003). Cdc42-dependent actin polymerization during compensatory endocytosis in Xenopus eggs. Nat. Cell Biol. *5*, 727–732.

Suetsugu, S., Hattori, M., Miki, H., Tezuka, T., Yamamoto, T., Mikoshiba, K., and Takenawa, T. (2002). Sustained activation of N-WASP through phosphorylation is essential for neurite extension. Dev. Cell *3*, 645–658.

Taunton, J., Rowning, B.A., Coughlin, M.L., Wu, M., Moon, R.T., Mitchison, T.J., and Larabell, C.A. (2000). Actin-dependent propulsion of endosomes and lysosomes by recruitment of N-WASP. J. Cell Biol. *148*, 519–530.

Tian, L., Nelson, D.L., and Stewart, D.M. (2000). Cdc42-interacting protein 4 mediates binding of the Wiskott-Aldrich syndrome protein to microtubules. J. Biol. Chem. *275*, 7854–7861.

Torres, E., and Rosen, M.K. (2003). Contingent phosphorylation/dephosphorylation provides a mechanism of molecular memory in WASP. Mol. Cell *11*, 1215–1227.

Volkman, B.F., Prehoda, K.E., Scott, J.A., Peterson, F.C., and Lim, W.A. (2002). Structure of the N-WASP EVH1 domain-WIP complex: insight into the molecular basis of Wiskott-Aldrich Syndrome. Cell *111*, 565–576.

Yin, H.L., and Janmey, P.A. (2003). Phosphoinositide regulation of the actin cytoskeleton. Annu. Rev. Physiol. *65*, 761–789.

Accession Numbers

Nucleotide and protein sequences for human and *Xenopus tropicalis* Toca-1 have been deposited in GenBank under the accession numbers AY514449 and AY640054, respectively.